

Original Article

# Thermo-Economic Analysis of Humidification-Dehumidification Desalination System Using Solar Energy

Degefa Legesse<sup>1</sup>, Kumara Thanaiah<sup>2</sup>

<sup>1,2</sup>Department of Mechanical Engineering, Bule Hora University, Bule Hora, Ethiopia.

<sup>1</sup>Degefa1221@gmail.com

Received: 03 January 2025; Revised: 05 February 2025; Accepted: 12 March 2025; Published: 31 March 2025

**Abstract** - The present study aimed to assess the energy and economic analysis of Paddy grass-based Humidification-Dehumidification Desalination (PHDD) using solar energy. The experimental setup of the humidifier and dehumidifier was fabricated to maintain the humid climatic conditions of the study area. Theoretical analysis of each component of the system was studied and compared with laboratory results. The performance of the PHDD system was evaluated by studying various physical parameters such as solar collector area, reservoir water tank volume, and temperature of the water reservoir. The cost-benefit analysis of the system was carried out by considering the amount of potable water production, the amount of energy consumed, and the components cost by comparing them with other desalination methods. The results revealed that irrespective of the paddy grass area, the volume of the storage water tank below and above 40 L is considered as optimal. The cost analysis of the present work proved the system could function with low maintenance cost when compared to other similar studies, and the price of the yield comes to around 19\$/m<sup>3</sup>. The solar collector area has a significant influence in augmenting the water yield. The optimal ratio of the water reservoir to the collector area is found to be around 13 L/m<sup>3</sup>.

**Keywords** - Dehumidification, Desalination, Humidification, Paddy grass packing material, Solar energy.

## 1. Introduction

Although over 71 % of the globe's area is enclosed with water, nearly 97.5 % of the water is saline in nature and comprises an enormous quantity of salt [1]. Consequently, the desalination technique is a more promising solution to solve the shortage of fresh water. There are many desalination techniques, such as Multi Effect Desalination (MED), Multi-Stage Flash (MSF), Reverse Osmosis (RO), Nano Filtration (NF), and Electro Dialysis (ED), which consume a lot of energy.

Half of the whole world's desalination capacity is placed in the Middle East, Persian Gulf and Northern African regions. Major desalination plants are available in Saudi Arabia and have achieved the number one position in the World desalination capacity, and approximately 15,906 desalination plants are working all over the world, accounts 95.37 million m<sup>3</sup>/day from 177 countries [2]. At the end of 2017, nearly 50 percent of the plants were RO-established techniques. However, RO technology is dependent on high-pressure energy and also has maintenance issues [3].

Renewable energy sources such as solar desalination are a favorable method for the production of freshwater due to low-grade heat sources. In this view, the solar-driven humidification-dehumidification technique is considered a favorable technique [4, 5]. As per this technique, saline water is heated from the solar energy and moisture is added to the air (Humidification). Then, humidified air is made to flow through the dehumidifier, where cold water is circulated indirectly to remove the moisture from the air (Dehumidification) and finally, fresh water is produced.



## 2. Literature Review

In this research work, it is important to review, discover, and understand the earlier work carried out in a specific area. Similarly, technical assessment of the experimental work and mathematical modeling on Humidification-Dehumidification (HDH) using solar collectors from the various available papers are listed in Table 1.

**Table 1. Summary of the work on the experimental study of HDH units with solar collectors**

Year	Author(s)	Brief title	Key Findings
2022	[6]	Parametric analysis of HDH desalination powered by photovoltaic system	Thermo-economic analysis was investigated along with new packing material in a dehumidifier. They found that improved is called Gain Output Ratio (GOR) for the system.
2022	[7]	Performance study of humidifier packing for HDH desalination	Experimental and theoretical work is carried out and optimized with 15 packing materials by using Scilab simulation software.
2013	[8]	Solar desalination based on multiple effect humidification process: experimental validation	The experimental setup was based on an HDH unit that was designed and tested at Sfax, Tunisia. Theoretical model was established to investigate the thermal performance using C++ programming and validated with experimental results.
2014	[9]	Solar desalination system using humidification-Dehumidification process	The Experimental investigation was carried out and conducted at Makkah using solar collectors for different weather conditions. They are able to produce 1.6 liters of fresh water for one kWh of solar energy.
2016	[12]	Experiment study of multi-effect isothermal heat with tandem solar heat	A porous ball humidifier was used. A theoretical study was carried out based on mass and energy balance. The yield increased when the temperature increased from 60 °C to 90 °C.
2017	[14]	Experimental study of a solar desalination with HDH unit using a rotating surface	A rotating black surface is used to investigate the performance of the system. The yield was 9 liter/m <sup>2</sup> /day during the summer.
2018	[17]	Experimental and numerical evaluation of an HDH system driven by solar energy	An experimental and theoretical analysis with closed air and open water was conducted using solar energy in Chile. Measured values were used to optimize the design.
2016	[20]	Experimental and theoretical study on HDH unit	Theoretical model is obtained from mass and energy equations. The calculated results were in good agreement with the experimental results.
2018	[23]	Investigation of HDH-Adsorption	Mathematical modelling of HDH with adsorption, along with recirculation was carried out. The Maximum reached GOR was 10 from the multiple recirculation of brine.
2018	[25]	Experimental investigation of hybrid HDH unit	Experimental work on the HDH unit was integrated with solar energy by inserting baffles in the cooler. They found unit performance is improved with increasing water temperature and mass flow rate of air.
2015	[26]	Experimental work on hybrid HDH unit with A/C system	They found that freshwater production increases with an increase in specific humidity and mass flow rate of air.

The use of packing material in the humidifier is one of the attempts to increase the effectiveness of the desalination process using the HDH system. The humidification is carried out in the humidifier, in which packing materials are used to better interact with the air and water. That humidifier consists of bubble columns [28], packed bed towers [29], and spray towers [30].

### 2.1. A Research Gap

No studies have been performed so far in which baffle plates are placed in a dehumidifier along with new packing material (paddy grass), experimental work, or thermos-economic analysis for the HDH system. The present work includes the mathematical model for each component of the system to assess the performance.

## 3. Materials and Methods

### 3.1. Paddy Grass

Paddy grass, also known as rice straw, is the stalks and leaves of rice plants that are left over after the grain has been harvested. This is a generally accessible, non-contaminating material. Figure 1 shows the genuine image of paddy grass pressing material.



Fig. 1 Picture of the paddy grass (a) Two layers, and (b) Three layers.

#### 3.1.1. Assumptions

- The quantity of paddy grass utilized is 1600, each having a breadth of 0.005 m and a length of 0.4 m.
- The packing density of the paddy grass is  $157.07 \text{ kg/m}^3$  with a surface territory of  $10.05 \text{ m}^2$ .

### 3.2. Methods

The current work is carried out using two methods: an analytical and experimental analysis, which is carried out to assess the humidification and dehumidification processes.

### 3.3. Experimental Details

The experimental arrangement consists of two parts such as humidification and dehumidification parts. The humidification part involves various fittings like water circulating pumps, water sprayers, air blowers, and air heating sources. Dehumidification part involves a number of copper pipes and baffle plates in order to get the cooling effect and condense the air to produce fresh water.

#### 3.3.1. Working Procedure

In order to begin the humidification process, the air is initially drawn into the air chamber from the blower and heated using the air heater, as shown in Figure 2. Location 1, where temperature and humidity sensors are placed for measurement. There will be a reduction in the temperature of the air, resulting in increased moisture-adding capability [35]. The hot air is sent from the bottom part of the humidifier. The saline water is heated from the secondary heating source, which is located close to the top portion of the humidifier. The hot saline water is

sprinkled from the two sprayers over the paddy grass humidifier, which helps in better mixing of air and water, and finally, the air absorbs moisture and is humidified [36]. The unabsorbed extra water is accumulated in the water reservoir tank. The water pump is utilized to circulate the water in a closed cycle. The hot, humid air is sent to the dehumidifier, where the moisture content is condensed on the surface of copper coils and baffle plates placed inside the dehumidifier. Air velocity is measured with the help of an Anemometer, while water flow is measured using Rotameters. Psychrometers were placed at three various positions, such as the humidifier inlet and exit and at the exit of dehumidifier as shown in the Figure 2.

### 3.3.2. Experimental Components

- Heat source: The capacity of the air heater is 500 W, and the water heater is 10 kW.
- Humidifier: The addition of moisture content to air is done in a closed hollow humidifier having a square profile cross-section of 0.4 and a height of 1m.
- Dehumidifier: The removal of moisture content from the air is carried out in a dehumidifier with a V-shaped hollow conduit with various baffles inside the conduit and with the help of a copper coil.
- Baffle plates: Baffle plates having dimensions 0.3cm thickness and 16 cm length are welded inside the dehumidifier conduit to rise the condensation process. The total number of plates used is 6, with a gap of 16 cm between them.
- Water sprayer: The topmost part of the humidifier is kept with water sprayers in order to improve the interaction between air and water. Each sprayer contains 36 number of small holes with a 0.8 cm distance, which helps in breaking the liquid into small droplets.
- Storage tank: In order to supply the saline water continuously, a saline water reservoir tank with a 50-liter volume is provided.

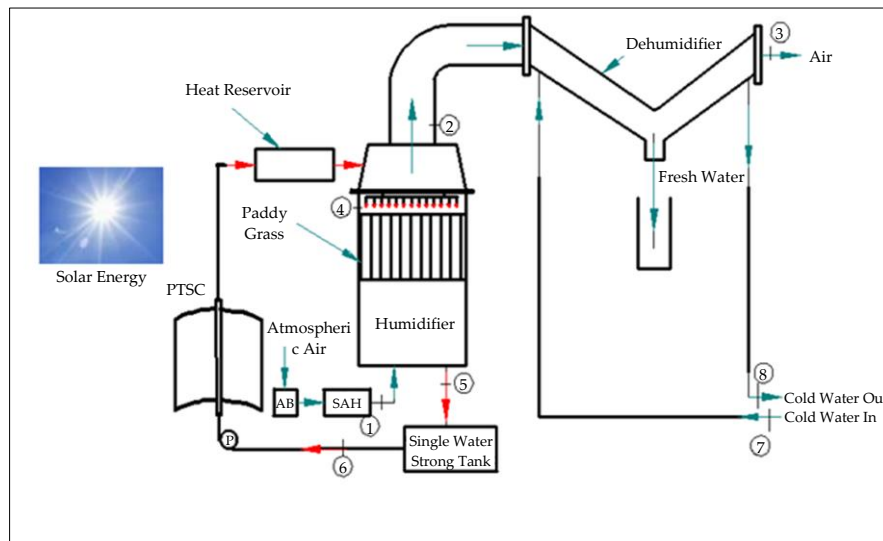


Fig. 2 Block diagram of the humidification dehumidification unit

- Air Blower: The air is drawn over the inlet air passage and is heated with the aid of an air heater and further directed to the air blower having a specification of  $500 \text{ m}^3/\text{hr}$  with inlet and outlet diameters of 7.5 and 8 cm. The supply of air is up to 50 meters with a velocity of 1000 rpm.
- Potable water collector: One-liter volume measuring container is kept under the dehumidifier unit.
- Thermocouples: The thermocouples utilized are of K-type with specifications of 0.3 cm diameter and 2 m length and in work range of -200 to 1200 °C with an accuracy of  $\pm 0.15 \text{ }^\circ\text{C}$  and uncertainty of 2%.
- Psychrometer: To examine the concentration of humidification, the dry, air-dry bulb and wet bulb temperature is measured.

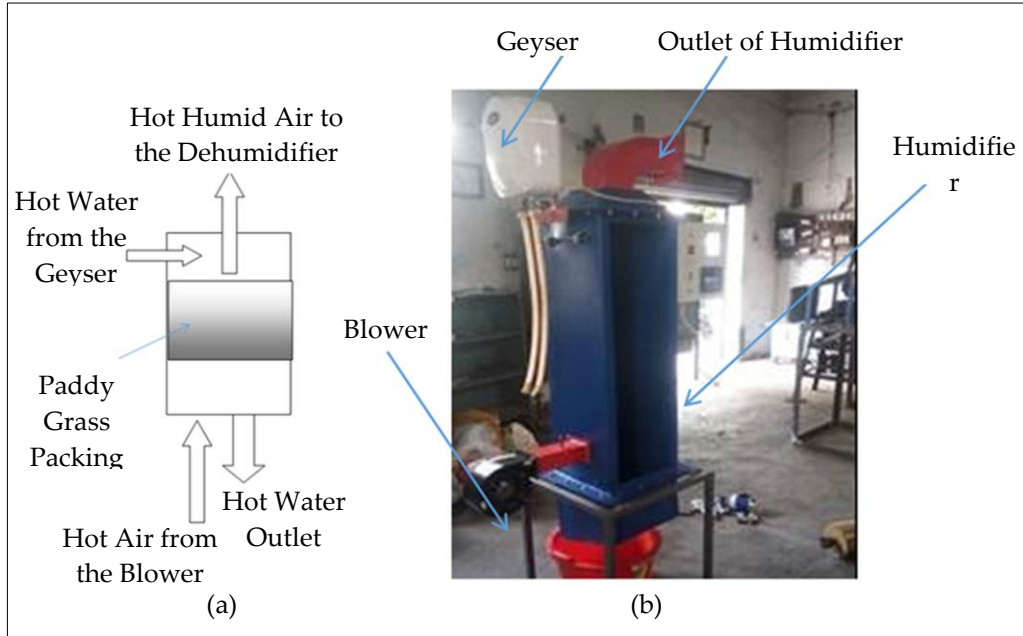


Fig. 3 Schematic view of (a) Humidifier with packing material, and (b) Experimental view with inlet duct to a humidifier, blower and water heat source.

### 3.4. Mathematical Modeling

#### 3.4.1. Solar Water Heater

In order to increase solar radiation utilization, a concentrated kind of collector, like a Parabolic Trough Solar Collector (PTSC), is used. PTSC contains a cylinder profile with a tubular receiver. The radiation absorbed [24] by the PTSC is given by

$$S = I_s \rho (Y\tau\alpha)_n K_{\tau\alpha} \quad (1)$$

Where  $I_s$  is the existing beam radiation reflectivity, and  $\tau\alpha$  is the product of transmittance absorptance. Convection and Radiation Heat loss is expressed using the following equation.

$$Q_{Loss} = \pi D_{co} L h_w ((T_{co} - T_a) + \epsilon_c \pi D_{co} L \sigma (T_{co}^4 - T_{sk}^4)) \quad (2)$$

Where  $h_w$  is the outside heat transfer coefficient,  $T_a$  is the ambient temperature, and  $T_{sk}$  is the sky temperature.

Radiative heat transfer loss: The radiative heat transfer from the receiver to the cover's inner surface is given by [37].

$$Q_{loss} = \frac{\pi D_o L \sigma (T_r^4 - T_{ci}^4)}{\frac{1}{\epsilon_c} + \frac{1 - \epsilon_c}{\epsilon_c} \left( \frac{D_o}{D_{ci}} \right)} \quad (3)$$

Where,  $D_o$  is the outer diameter of the receiver,  $D_{ci}$  is the cover inner diameter length of the collector,  $\sigma$  is Stefan-Boltzmann's constant,  $T_r$  is the receiver temperature,  $T_{ci}$  is the cover inner temperature, and  $\epsilon_c$  is the cover emissivity.

The conductive heat loss through the cover thickness is given by

$$Q_{loss} = \frac{2\pi k_c L (T_{ci} - T_{co})}{\ln \left( \frac{D_{co}}{D_{ci}} \right)} \quad (4)$$

Where  $k_c$  is the thermal conductivity,  $T_{co}$  is the cover's outer temperature, and  $D_{co}$  is the outer diameter.

The total heat loss is given by the following equation.

$$Q_{loss} = U_l A_r (T_i - T_a) \quad (5)$$

Where  $U_l$  is the overall heat transfer coefficient, and  $A_r$  is the receiver area.  $h_w$  is calculated using Nusselt number correlation for the flow of air along a tube in an outdoor environment as:

The useful energy gain is obtained by subtracting the total heat loss from the captured radiation expressed as

$$Q_u = F_R A_a [S - \frac{A_r}{A_a} U_l (T_i - T_a)] \quad (6)$$

Where  $F_R$  is the heat removal factor

The collector flow factor is written as follows:

$$F'' = \frac{F_R}{F'} = \frac{\dot{m}C_p}{A_r U_l F'} [1 - \exp(-\frac{A_r U_l F'}{\dot{m}C_p})] \quad (7)$$

Where  $F'$  is the Collector Efficiency factor is expressed as given below

$$F' = \frac{U_o}{U_l} \quad (8)$$

Useful energy gain in terms of collector inlet and outlet temperature is expressed as

$$Q_u = \dot{m}c_p(T_i - T_o) \quad (9)$$

Where  $T_o$  is the outlet temperature

The instantaneous solar collector efficiency is obtained from the following expression,

$$\eta_i = \frac{Q_{sl}}{I_s A_{sc}} \quad (10)$$

### 3.4.2. Water Storage Tank

The energy equations for the water storage tank are expressed as

$$m_{w1} c_{pw} \frac{dT_{w1}}{dt} = M_{w1}(t) c_{pw} T_{w2}(t) + M_{mw}(t) c_{pw} T_{mw}(t) - M_{w1} c_{pw} T_{w1}(t) - q_{1w1amb} \quad (11)$$

### 3.4.3. Solar Air Collector

The solar air heater was utilized for heating the inflow of atmospheric air to the humidifier. The energy balance equations for the solar air heater are as follows [38].

Second glass cover:

$$m_g c_{pg} \frac{dT_{g2}}{dt} = I_s \alpha_g A_{sc} + Q_{r,g1g2} - Q_{c,g2amb} - Q_{r,g2s} + Q_{c,g1g2} \quad (12)$$

For the first glass cover:

$$m_g c_{pg} \frac{dT_{g1}}{dt} = I_s \alpha_g A_{sc} \tau_g - Q_{r,g1g2} - Q_{c,g2a1} + Q_{r,pg1} - Q_{c,g1g2} \quad (13)$$

First air pass:

$$m_a c_{pa} \frac{dT_{a1}}{dt} = Q_{c,pa1} + Q_{c,g1a1} - M_a C_{pa} (T_{a1e} - T_{ai}) \quad (14)$$

Absorber plate:

$$m_p c_{pp} \frac{dT_p}{dt} = I_s \alpha_p \tau_g^2 A_c - Q_{cpa2} - Q_{c,pa1} - Q_{r,pg1} - Q_{r,pb} \quad (15)$$

Second air pass:

$$m_a c_{pa} \frac{dT_{a2}}{dt} = Q_{cpa2} + Q_{cba2} - M_a C_{pa} (T_{a2e} - T_{a1ep}) \quad (16)$$

Base plate:

$$m_b c_{pw} \frac{dT_b}{dt} = Q_{rpb} - Q_{cba2} - Q_{1batm} \quad (17)$$

### 3.4.4. Paddy Grass Humidifier

#### Overall Heat and Mass Transfer in the Paddy Grass Humidifier

In the paddy grass packing humidifier, hot saline water is sprayed from the top of the humidifier over the bundles of grass material while air flows from the bottom. In view of the large number of grasses that were filled in the humidifier, it is tough to model directly, so in order to simplify the problem, a counter-flow heat exchanger model is considered.

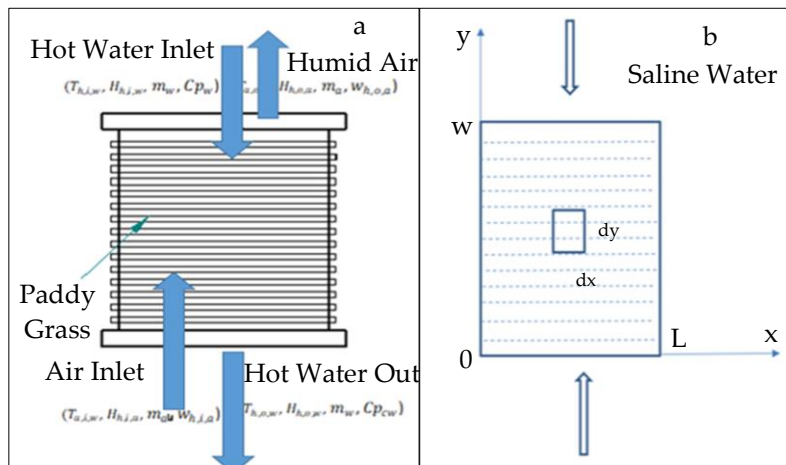


Fig. 4 Schematic of paddy grass humidifier (a) The diagram of the structure of module, and (b) Representation of model calculation.

During the humidification process, heat and moisture between saline water and the air are governed by the following equations:

$$\frac{\partial T_a}{\partial y} = \frac{h_{to} A_{to}}{m_a c_{pa} W} (T_s - T_a) \quad (18)$$

$$\frac{\partial w_a}{\partial y} = \frac{\rho_a k_{to} A_{to}}{m_a W} (w_s - w_a) \quad (19)$$

$$\frac{\partial T_s}{\partial x} = \frac{h_{to} A_{to}}{m_s c_{ps} L} (T_a - T_s) + \frac{\rho_a k_{to} A_{to} H_v}{m_s c_{ps} L} (w_a - w_s) \quad (20)$$

$$\frac{\partial X}{\partial x} = \frac{\rho_a k_{to} A_{to}}{m_s L} (w_s - w_a) \quad (21)$$

Where s stands for the solution and a for air, respectively,  $H_v$  is evaporation heat of vapor,  $w$  is humidity, and  $w_s$  is the phase equilibrium humidity of the air with the saline water at the concentration of  $X_s$  and the temperature of  $T_s$ .

$$w_s = 0.662 \frac{P_v}{P_{at} - P_v} \quad (22)$$

The boundary conditions for the mixture are

$$x=0, T_s = T_{si}, w_s = w_{si} \quad (23)$$

$$y=0, T_a = T_{ai}, w_a = w_{ai} \quad (24)$$

The total resistance consists of three components such as solution component, air component and paddy grass component. Heat transport and mass transport are written as follows:

$$\frac{1}{h_{to}} = \frac{1}{h_s} + \frac{d}{K} + \frac{1}{h_a} \quad (25)$$

$$\frac{1}{k_{to}} = \frac{1}{k_s} + \frac{d}{D} + \frac{1}{k_a} \quad (26)$$

Where d is the diameter of the paddy grass, K is the thermal conductivity, and D is the moisture diffusivity.

The convective heat transfer coefficient (h) and mass transfer coefficient (k) of the air and saline water are denoted by the Nusselt number and Sherwood number and written as follows:

$$N_u = \frac{hd}{K} \quad (27)$$

$$S_h = \frac{kd}{D} = \frac{N_u}{Le^{\frac{1}{3}}} \quad (28)$$

Where K is the heat conductivity, Le is the Lewis number, and D is the diffusivity.

The effect of this paddy grass on the system performance is the major focus of this research, and its characteristics depend on the moisture diffusivity (D), heat diffusivity (K) and the capacity of volume of the humidifier. These are the parameters to be examined in this work. Furthermore, the area of the paddy grass was also investigated. Reynold's number for air and solution across the grass tubes is far below 2300. Therefore, air and solution may be considered as a laminar flow. Hence, the following equation can be used as a fully developed laminar heat transfer around the tubes.

Nusselt number of air stream are expressed as [39]

$$N_{ua} = 1.13 c_1 Re_{do,max}^m Pr_a^{0.33} \quad (29)$$

Where  $c_1$  and m are constants and are calculated using the following table [39].  $Pr$  is the Prandtl number and  $Re_{do,max}$  is calculated using:

$$Re_{do,max} = \frac{u_{a,max} d_o}{\gamma_a} \quad (30)$$

The pressure drop of the solution for laminar flow around the paddy grass is given by

$$\Delta P_{SH} = \frac{64}{Re_s} \frac{L_H}{d} \frac{\rho_s U_s^2}{2} \quad (31)$$

Flow characteristics for air stream have been investigated by and used presently in this study, and they are given as follows:

$$f_a = a R_e^{-b} \quad (32)$$

$$N_{ua} = c Re_a^m Pr_a^{\frac{1}{3}} \quad (33)$$

$$Sh_a = D Re_a^n Sc_a^{\frac{1}{3}} \quad (34)$$

The constants a, b, c, D, m and n are obtained from the geometric configurations of the paddy grass humidifier. The applicability of these correlations is for the Reynold numbers up to 500 and the module Packing Fraction (PF) 0.2 to 0.6. Therefore, in this research, the Reynold number is 210, and the PF is 0.512. Hence, the above correlations can be used in this research. The constants are a=4.299, b=0.363, C=1.98, m=0.443, D=3.402 and n=0.374. Sc is the Schmidt number, and Pr is the Prandtl number, respectively.

The pressure drop across the air stream in the humidifier is given by,

$$\Delta P_{aH} = f_a N_l \left( \frac{1}{2} \rho_a U_{amax}^2 \right) \quad (35)$$

Where,  $N_l$  is the number of grass fibres in the humidifier and it is equal to 1600 in this work.

$$U_{amax} = \frac{P_t}{P_t - d} U_a \quad \text{When } P_d > (P_t + d)/2 \quad (36)$$

$$U_{amax} = \frac{P_t}{2(P_d - d)} U_a \quad \text{When } P_d < (P_t + d)/2 \quad (37)$$

In order to analyze the heat transfer and mass transfer properties of the paddy grass humidifier, two terms are defined known as latent effectiveness and sensible effectiveness as follows:

$$\eta_{lat} = \left[ \frac{w_{ao} - w_{ai}}{w_{si} - w_{ai}} \right] \quad (38)$$

$$\eta_{sen} = \left[ \frac{T_{ao} - T_{ai}}{T_{si} - T_{ai}} \right] \quad (39)$$

### 3.4.5. Dehumidifier

The dehumidifier component in the HDH unit is a fin-tube kind of heat exchanger. Indirect contact between hot, humid air and feed water takes place through the gap between fins and tube. The shape of the humidifier is a V-shape hollow structure, one end of which hot humid air enters and leaves from the other end.

As reported [40] in the literature polymeric solid hollow fibre type heat exchanger is efficient when compared to shell and tube.

To study the performance of the dehumidification process in the dehumidifier, the  $\epsilon$ -NTU method is implemented.

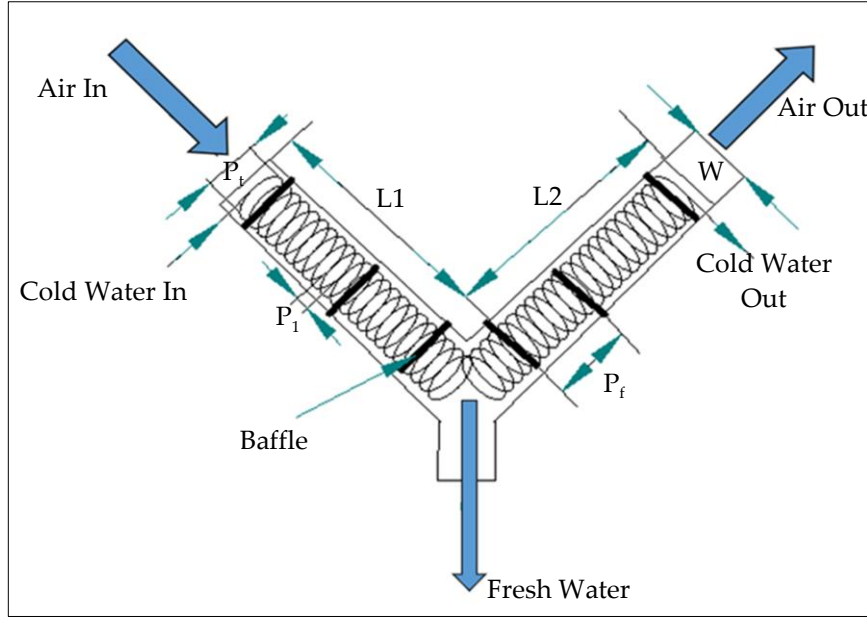


Fig. 5 Schematic drawing of the dehumidifier

The effectiveness can be written as

$$\varepsilon = 1 - \exp \left\{ \frac{NTU^{0.22}}{C_R} - [\exp(-C_R NTU^{0.78}) - 1] \right\} \quad (40)$$

Where

$$NTU = \frac{UA}{m_a c_{pa}} \quad (41)$$

$$C_R = \frac{m_a c_{pa}}{m_c c_{pc}} \quad (42)$$

The total heat resistance ( $1/UA$ ) is expressed as

$$\frac{1}{UA} = \frac{1}{h_i A_i} + R_{wl} + \frac{1}{\eta_f h_a A_a} \quad (43)$$

Where, the middle term of the right hand side of the equation  $R_{wl}$  is the resistance of the wall and  $\eta_f$  is the efficiency of the fin,  $A_i$  is the inner surface area of the copper tube and  $A_a$  is the heat exchanger area in the air side. The first and last terms of the right hand side of the equation are tube side resistance and air side resistance, respectively.

During the experimental work, the cold water flow rate is 0.05 kg/s, and the corresponding Reynolds number is 15300, which is more than 4000. Therefore, flow is considered to be turbulent. Hence, the convective heat transfer coefficient of the water  $h_i$  in the expression (26) can be calculated from the following expression.

$$h_i = \left( \frac{K_i}{D_i} \right) \frac{(R_{e_{Di}} - 1000)(F_i/2)P_r}{1.07 + 12.7 \sqrt{F_i/2(P_r^{0.7} - 1)}} \quad (44)$$

$$F_i = \frac{1}{\left( 1.58 \ln R_{e_{Di}} - 3.28 \right)^2} \quad (45)$$

The heat transfer coefficient  $h_a$  for the air side of the dehumidifier is expressed with:

$$h_a = j \frac{m_a c_{pa}}{P_r^{2/3}} \quad (46)$$

$$j = 0.4 R_{edc}^{-0.468+0.04076N_r} \left( \frac{A_o}{A_{po}} \right)^{0.159} N_r^{-1.261} \quad (47)$$

Where,  $m_a$  the mass flow rate of through fins,  $A_o$  is the external surface area of the tubes, and  $A_{po}$  is the total heat exchange area, respectively.

**Performance Indices:** In order to assess the performance of the system, three parameters are defined, and they are as follows:

#### 3.4.6. Gain Output Ratio (GOR), Coefficient of Performance (COP) and Electric COP ( $COP_E$ ):

The ratio of latent heat of evaporation to total heat supplied to the desalination unit is called the Gain Output Ratio (GOR). GOR is an important performance parameter used for humidification and dehumidification processes. It describes the energy evaluation of the desalination plant and all other thermal desalination techniques.

$$COP = \frac{AP \cdot H_w}{\int (q_{solar} + w_{pump} + w_{blower}) dt} \quad (48)$$

Where  $H_w$  is the latent heat of condensation of water, AP System capacity.

Similarly,

$$COP_E = \frac{AP \cdot H_w}{\int (w_{pump} + w_{blower}) dt} \quad (49)$$

Where  $w_{pump}$  and,  $w_{blower}$  are the power consumption of pump and blower respectively and are expressed as

$$w_{pump} = \frac{m_s \Delta P_s}{\rho_s \eta_{pump}} \text{ and } w_{blower} = \frac{m_a (\Delta H_{ah} + \Delta H_{ad})}{\rho_s \eta_{blower}} \quad (50)$$

Where,  $\eta_{blower}$  and  $\eta_{pump}$  are efficiencies of the blower and pump, respectively.

The power spent by the electric heat source to enhance the temperature of the water flowing through the humidifier paddy grass can be calculated using.

$$w_{ewh} = c_{pw} m_w (T_{wo} - T_{wi}) \quad (51)$$

Similarly, for air heater,

$$w_{eawh} = c_{pa} m_a (T_{ao} - T_{ai}) \quad (52)$$

Instantaneous freshwater production (IP) and Accumulated water production (AP) are well-defined as

$$IP = m_a (\omega_{dai} - \omega_{da0}) \quad (53)$$

$$AP = \int m_a (\omega_{dai} - \omega_{da0}) dt \quad (54)$$

Where  $\omega_{dai}$  and  $\omega_{dao}$  are moisture content at the in and out of the dehumidifier. Specific Energy Consumption (SEC): Specific energy consumption is the amount of fresh water produced per unit volume of water.

$$SEC = \frac{\rho_w \int (w_{pump} + w_{blower}) dt}{AP} \quad (55)$$

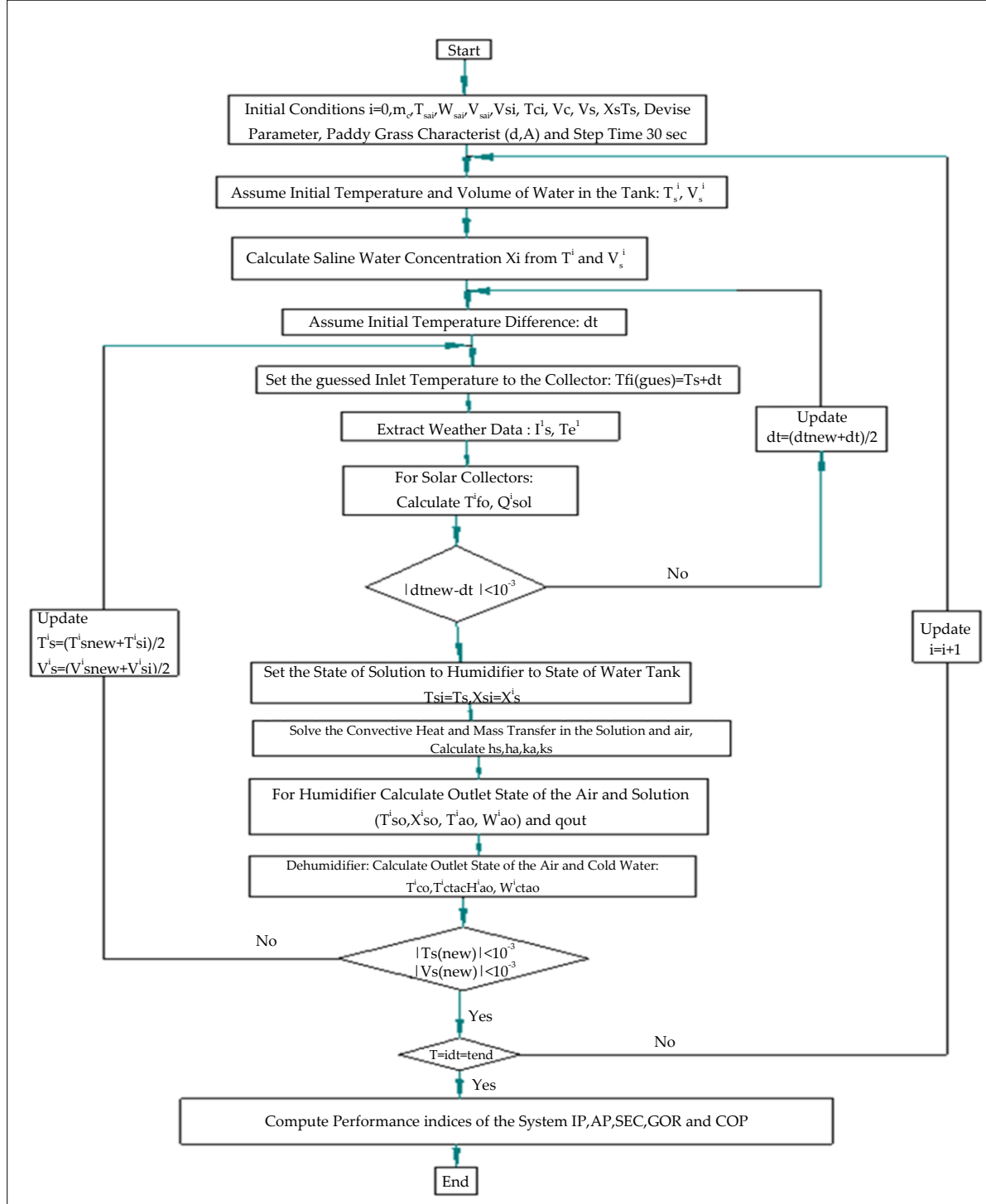


Fig. 6 Flow chart for the solution method in simulation for the entire system

### 3.5. Calculation Procedure

The comprehensive solution method is presented in the flow chart, as shown in Figure 6.

1. Inlet operational conditions such as mass flow rate, freshwater volume collected, inlet temperature, humidity (input and output states), the mass flow rate of air, saline water, the concentration( $x$ ), the equipment parameter such as solar collector, humidifier, dehumidifier, water reservoir tank etc.
2. Assume initial values of the temperature and volume of the saline water inside the saline water reservoir tank ( $T_s^i, V_s^i$ )
3. The saltwater concentration is computed from the entire mass of the NaCl and the volume of the reservoir tank at temperature.
4. Initial temperature difference ( $dt$ ) is assumed.
5. Guess the set inlet temperature ( $T^i$ ) to the water collector reservoir as ( $T^i + dt$ ). Take the solar intensity data and atmospheric temperature. Equations (1)-(10) are used to compute the outlet temperature of the solar collector, energy received from the collector and its efficiency.
6. Compute heat reservoir temperature. Now, estimate fresh temperature difference, and if there is a deviation within the limit, then go to step 7, or else assign and go to step 5 until convergence is achieved.
7. The inlet temperature and concentration of the humidifier are equivalent to the present solution temperature and concentration in the heat reservoir tank. Now, compute the Equations (18)-(28) for the humidifier and estimate the outlet temperature and saltwater concentration from the humidifier. Compute the air temperature and humidity for the humidifier. Finally, compute the exit heat load.
8. Taking the exit temperature, the humidity of air from the humidifier is used as an input temperature, and air humidity is used as input to the dehumidifier. Compute the Equations (39)-(47) to obtain the exit temperature, humidity and enthalpy of the air coming out of the dehumidifier. Compute the output cooling water temperature of the dehumidifier.
9. Equations are used to solve the temperature and volume of the heat storage reservoir. If the computed and initial assumed values are within the limit, then move to step (10) or consider the average of these values and move to (3) till it converges.
10. Now, move to time interval  $i=i+1$  and send back to (2) till the expected time is achieved. Finally, compute the performance parameters.

## 4. Results and Discussion

### 4.1. Model Validation

The theoretical present model outputs are compared with the experimental outputs in order to verify the validity. Many influencing parameters [42] available from the previous literature work are considered in this work as well. These are inlet saline water, air flow rates into the humidifier unit and the packing fractions. The specification of the humidifier is a square cross-section of 0.40 m by 0.40 m, the flow rate of the saline water is 0.04 kg/s, the inlet flow rate is 0.004 kg/s at 35 °C, and the relative humidity is 60 %.

The initial saline water temperature of the storage take was fixed at 40 °C with a concentration of 3.5 % and a capacity of 90 L. The cold water flow rate to the dehumidifier is 0.04 kg/s. The experiment was done on 12<sup>th</sup> August 2018 and measured solar radiation and atmospheric temperature at Surathkal, India, which is represented in Figure 7.

As it is seen (Figure 8), the understanding between the determined and the experimental outputs is acceptable. The relative deviations between the determined and the tried estimations of  $T_s$  and accumulated production within are 2% and 4.5%, respectively, as shown in Figure 8. Accordingly, the theoretical model is valid and could be utilized to examine the performance.

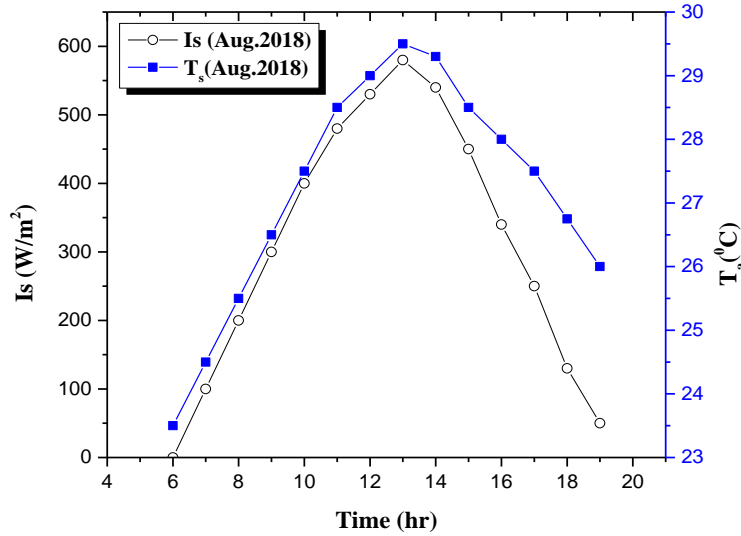


Fig. 7 Solar radiation and atmospheric temperature against time duration on a typical day in August 2018. at Surathkal, India.

#### 4.2. Experimental and Computational Results

To evaluate the production of fresh water and paddy grass humidifier outlet temperature, measured inlet water and air temperature are used as input values to the numerical model. To confirm the model, a reasonable study was carried out between mathematical modeling and experimental results, which is shown in Table 2.

The maximum variation for the above performance indices is 6.1%. As observed in Figure 8, the variations are less than 2% for tank water temperature. The variation of measured and experimental values are within 5% and 6% for latent effectiveness and sensible effectiveness, respectively, as shown in Figure 9. Therefore, the theoretical mathematical model can be used to analyze the system performance for the three different cases: paddy grass packing, polypropylene, and without packing. Paddy grass packing properties, namely moisture diffusivity, thickness, and area, are considered in detail in the study.

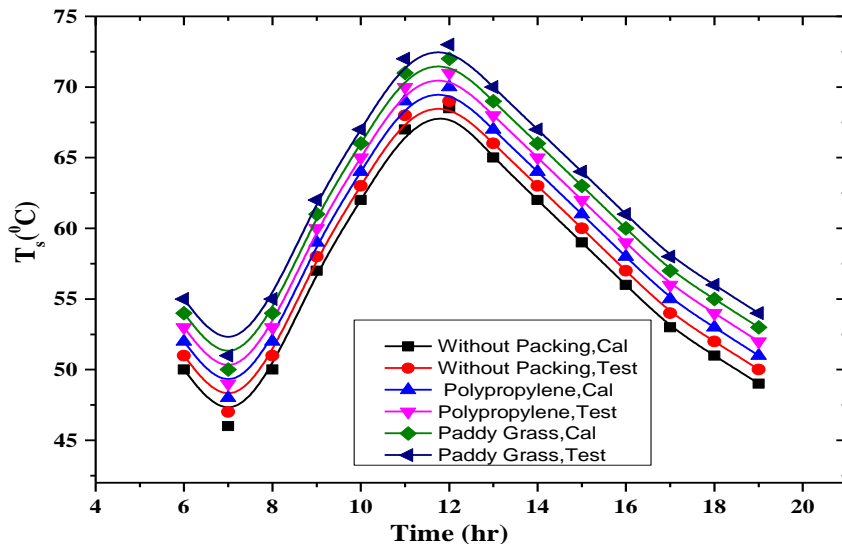


Fig. 8 Tested and calculated water tank temperature for different two different packing

**Table 2. Calculated and measured system performance during the operation of the packing materials**

Packing material	$AP_{cal}$ (kg/day)	$AP_{tes}$ (kg/day)	Error (%)	$SEC_{cal}$ (kWh/m <sup>3</sup> )	$SEC_{tes}$ (kWh/m <sup>3</sup> )	Error (%)	COP (cal)	COP (Test)	Error (%)
Paddy grass	7.35	7.14	2.91	22	21	4.5	0.65	0.61	5.3
Polypropylene	4.65	4.23	4.2	23	22	4.3	0.4	0.37	5.2
Without packing	3.5	3.3	5.7	20	21	4.7	0.3	0.28	6.1

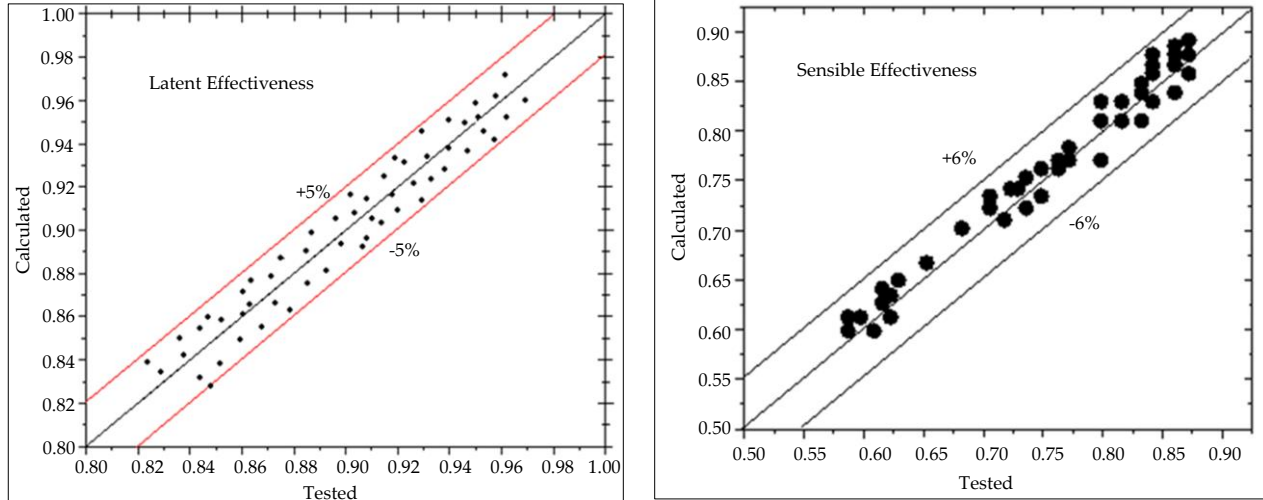


Fig. 9 The deviancy between the experimental and calculated latent effectiveness and sensible effectiveness (a) Latent effectiveness, and (b) Sensible effectiveness.

#### 4.3. Solar Collector Performance

The solar collector is one of the significant components of the HDHD system. The maximum amount of energy is collected from this element. Accordingly, the evaluation of the collector on the performance is important for the whole system. Hence, the degree of its performance is the collector efficiency, which is given in Equation (56) and is well-defined as useful solar energy collected over a period of time to available solar radiation. Under these conditions, the instantaneous collector efficiency is plotted as a linear function of the term  $(T_{fi} - T_a)/I_s$ :

$$\eta_i = 0.64 - 2.44(T_{fi} - T_a)/I_s \quad (55)$$

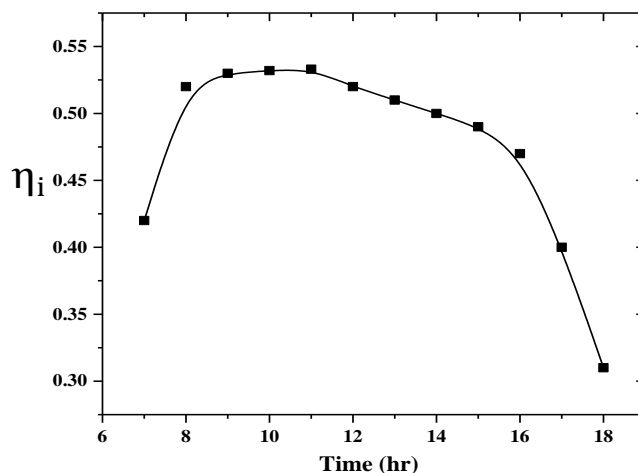


Fig. 10 Variation of instantaneous collector efficiency with time

From the above equation, the maximum efficiency of the collector will reach 64 when the second term of the right-hand side is zero, which means the water collector's temperature is the same as that of the atmospheric temperature. Hence, the u-tube evacuated collector has better performance efficiency than plate collectors [43]. The instantaneous collector efficiency with the time is shown in Figure 10.

The variation of efficiency is from 0.35 to 0.52 and attains a peak at about 10 am (nearly 80 percent of the noon period) because the solar energy is nearly  $450 \text{ W/m}^2$  whereas the change in the temperature  $T_f$  and  $T_a$  is not very high. Consequently, the ratio of temperature difference to  $I_s$  is very low and hence, efficiency reaches the highest value.

#### 4.4. Effect of Saline Water Volume in the Storage Tank

The simulation of a saline water tank is carried out for different volumes of water. Initially, the system is operated with a saline water temperature of  $50^\circ\text{C}$  starting at 6 am till the temperature is lower than  $50^\circ\text{C}$  during the afternoon. The optimum collecting area is  $4.2 \text{ m}^2$ .

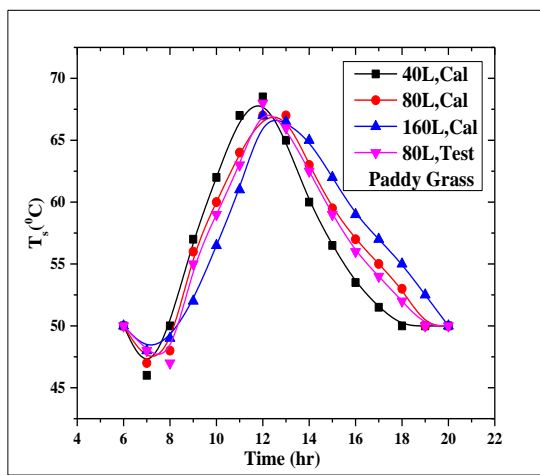


Fig. 11 Effect of tank volume on the water temperature in the water tank through the working time

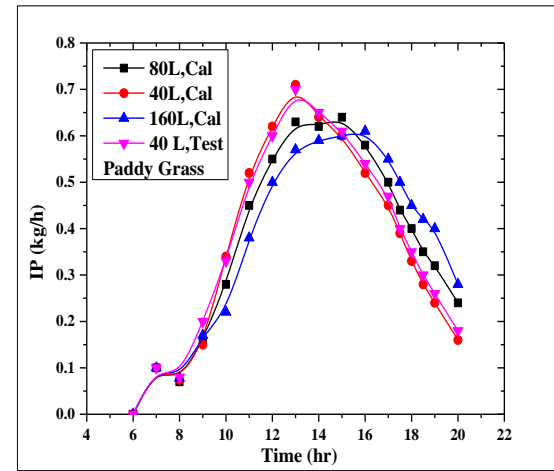


Fig. 12 Effect of tank volume on the instantaneous water production through the working time

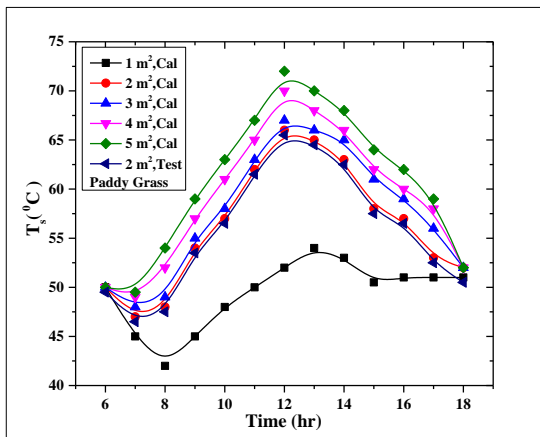


Fig. 13 Effect of solar collector area on the water temperature in the water tank through the working time

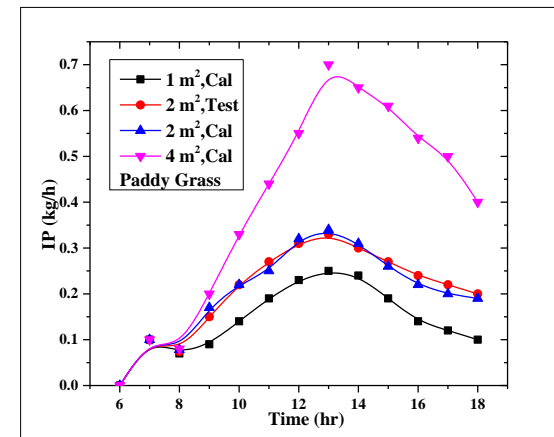


Fig. 14 Effect of collector area on the instantaneous water production through the working time

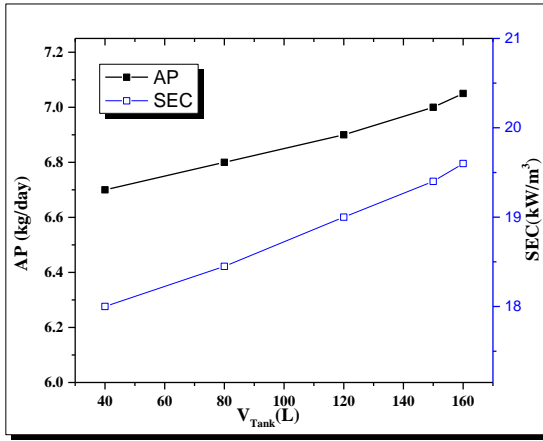


Fig. 15 Variation of accumulated fresh water production with tank water volumes

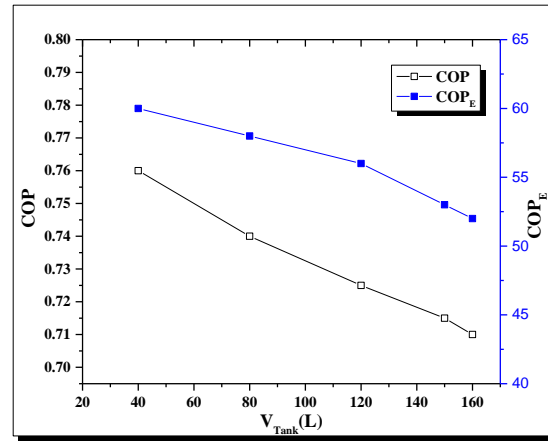


Fig. 16 Variation of coefficient of performance with tank water volumes

#### 4.5. Effects of Solar Collector Areas

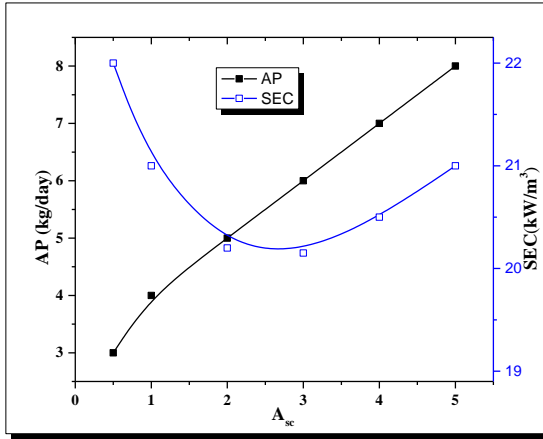


Fig. 17 Variation of accumulated fresh water production with solar collector area

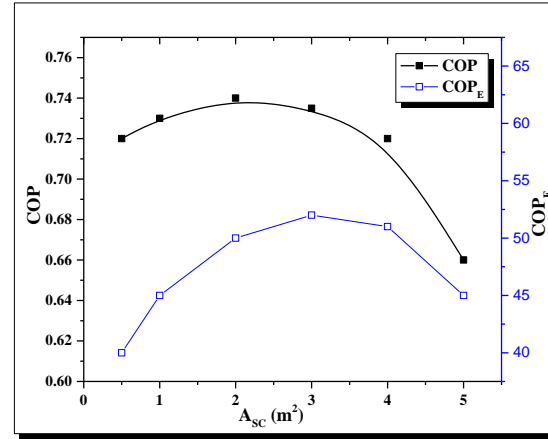


Fig. 18 Variation of coefficient of performance with solar collector area

#### 4.6. Economic Evaluation

Economic factors play a vital part in finding the projected desalination system decision. An economic calculation is carried out to know the final cost for the water yield.

Considering that the necessary cost for the desalination system is borrowed from the bank, yearly interest payment for the principal cost is calculated from the product of principal cost and the amortization factor  $a$  and is expressed as:

$$a = \frac{i(1+i)^n}{(1+i)^n - 1} \quad (56)$$

Where  $i$  is the yearly interest rate,  $n$  is the lifespan period of the system. The parameters and assumptions made for the economic calculation are listed in Table 3.

Table 3. Factors used in calculation of economic investigation

Factors	Unit	Value
System capacity (AP)	kg/day	7
SEC	kW/m <sup>3</sup>	20

System availability (F) [3]		0.9
Life span (n) [3]	year	20
Interest Rate (i) [44]	-	5%
Amortization Factor (a)	-	0.08

The working conditions are a 40 L storage saline water tank, a 4 m<sup>2</sup> collector area and a paddy grass humidifier. Under these conditions, the AP is 7 kg/day. The specific energy consumption is 20 kWh/m<sup>3</sup>, which indicates that the electrical energy utilization is very less compared to traditional desalination systems like multistage flash and reverse osmosis [45, 46]. The consumption of electrical energy rate at Surathkal as of 2018 is 0.2 \$/kWh. The yearly principal and operational cost ( $A_{Cost}$ ) is the sum of the yearly direct principal cost ( $A_{Fixed}$ ) and yearly operational and maintenance cost ( $A_{OM}$ ) is expressed as:

$$A_{Cost} = (A_{Fixed} + A_{OM}) \quad (57)$$

$$A_{Fixed} = a(C_{Fixed}) \quad (58)$$

$$A_{OM} = (A_{Elec} + A_{Paddy} + A_{Maita}) \quad (59)$$

$$A_{Maita} = (0.2 \times A_{Fixed}) \quad (60)$$

Where  $C_{Fixed}$  the whole asset of the system is,  $A_{Paddy}$  is the paddy grass replacement price, bearing in mind that fouling is due to salt.  $A_{Elec}$  and  $A_{Maita}$  are the yearly electricity price and yearly maintenance price, respectively. The water production price of the system can be expressed as:

$$WPC = \frac{A_{Cost}}{(AP \times F \times 365)} \quad (61)$$

Where F is the system availability and its value is 90 percent per annum [3, 44].

Fixed cost, operational cost and WPC are tabulated in Table 4. The table shows that the solar collector price adds to nearly 60 % of the entire price of the system. The yearly operational and maintenance price is about 30 % of the entire water production price, and the final price of the water production is 19 \$/m<sup>3</sup>, which is similar to the other small-capacity desalination system.

Table 4. The results of cost for principal investment, operational and maintenance

Part	Unit cost	Quantity	Approximate cost
Fixed cost			
Blower	35\$	1	35\$
Pump	30\$	2	60\$
Humidifier	50\$	1	50\$
Paddy grass	0.5\$	10.7 m <sup>2</sup>	5.3\$
Dehumidifier	80\$	1	80\$
Pipe fittings and instruments	25\$	-	25\$
Solar collector	100\$/m <sup>2</sup>	2	200\$
Storage tank	900\$/m <sup>3</sup>	0.05	40\$
<b>Total fixed cost (<math>C_{Fixed}</math>)</b>			495.3\$/year
<b>Yearly Fixed cost (<math>A_{Fixed}</math>)</b>			99\$/year
OM cost			
Electrical energy cost	0.2 \$/kWh	73 kWh/year	14.6

Paddy grass replacement ( $A_{Paddy}$ )	10 % per annum	10\$	1\$/year
Maintenance ( $A_{Maita}$ )			15.6\$/year
Yearly OM cost ( $A_{OM}$ )			31.2\$/year
$A_{Cost}$			130.2\$/year
WPC			19\$/m <sup>3</sup>

Table 5. Final cost of the water and comparison with other desalination system

Year	Desalination process	Energy source	Humidifier area	Production (L/day)	WPC (\$/m <sup>3</sup> )	Ref.
2011	ED-PV	25 kWp PV	-	10000	2.38	[48]
1998	MED-solar	38 m <sup>2</sup> -solar collector area	-	505	80	[49]
2017	HDH	Waste heat and electric energy	14 m <sup>2</sup>	15	10	[50]
2006	MSF	Steam and electric energy	-	5000	2.66	[47]
2005	Solar still	3 m <sup>2</sup> -basin area	-	7.5	50	[46]
2020	HDH	Solar energy	Paddy grass-10.7 m <sup>2</sup>	13	19	Present work

## 5. Conclusion

The availability of fresh water in isolated and dry regions is scarce. The desalination technique is an excellent solution to overcome the scarcity of fresh water. Conventional techniques are well-suited for large-scale production. However, affordable and efficient potable water production methods have become a challenging issue, especially in remote parts of the world. In this view, the HDH process is considered a promising desalination technique for producing potable water in remote areas. The viability of solar energy-based and paddy grass humidification dehumidification systems has been investigated in the present work. A theoretical mathematical model was established for each component of the system. These are the inferences generated from energy and economic analysis.

- The thermal energy reservoir is a significant part of resolving the variation in solar radiation. So, the system can operate when there are fewer hours of sunshine and during the nighttime. Irrespective of the paddy grass area, the volumes of the storage water tank below and above 40 L are not considered as optimal.
- The solar collector area was also significant in augmenting the accumulated water yield. In the present study, the optimal ratio of tank volume to area is found to be around 13 L/m<sup>2</sup>.
- The cost analysis of the present work proved the system could have functioned with a low maintenance cost; when compared to other similar studies, the price of the yield comes to around 19\$/m<sup>3</sup>. Hence, this technology is suitable for smaller communities with acceptable price costs.

Paddy grass materials can be selected as a substitute for artificial materials to achieve a high production rate and cost-effective and reliable operation of humidification and dehumidification desalination plants. The solar collector's price is higher when compared to other units of the system, and if it is minimized with the forthcoming research work, then the water production cost will come down considerably.

### 5.1. Future Work

1. Usage of geothermal energy sources or biomass energy sources may result in constant and better yield compared to the solar HDH technique.
2. HDH desalination process, with paddy grass as packing material, may be adopted for wastewater treatment in coffee processing plants.
3. The present research can be extended using nanoparticles with different volume fractions to increase heat transfer rate and system yield.

## References

- [1] A.E. Kabeel et al., "Water Desalination Using a Humidification-Dehumidification Technique-A Detailed Review," *Natural Resources*, vol. 4, no. 3, pp. 286-305, 2013. [[CrossRef](#)] [[Google Scholar](#)] [[Publisher Link](#)]
- [2] Edward Jones et al., "The State of Desalination and Brine Production : A Global Outlook," *Science of The Total Environment*, vol. 657, pp. 1343-1356, 2019. [[CrossRef](#)] [[Google Scholar](#)] [[Publisher Link](#)]
- [3] Fawzi Banat, and Nesreen Jwaied, "Economic Evaluation of Desalination by Small-Scale Autonomous Solar-Powered Membrane Distillation Units," *Desalination*, vol. 220, no. 1-3, pp. 566-573, 2008. [[CrossRef](#)] [[Google Scholar](#)] [[Publisher Link](#)]
- [4] K. Zhani, and H. Ben Bacha, "Experimental Investigation of a New Solar Desalination Prototype Using the Humidification Dehumidification Principle," *Renewable Energy*, vol. 35, no. 11, pp. 2610-2617, 2010. [[CrossRef](#)] [[Google Scholar](#)] [[Publisher Link](#)]
- [5] A.E. Kabeel, and E.M.S. El-Said, "Applicability of Flashing Desalination Technique for Small Scale Needs Using a Novel Integrated System Coupled with Nanofluid-Based Solar Collector," *Desalination*, vol. 333, no. 1, pp. 10-22, 2014. [[CrossRef](#)] [[Google Scholar](#)] [[Publisher Link](#)]
- [6] He Weifeng et al., "Parametric Analysis of Humidification Dehumidification Desalination Driven by Photovoltaic/Thermal (PV/T) System," *Energy Conversion and Management*, vol. 259, 2022. [[CrossRef](#)] [[Google Scholar](#)] [[Publisher Link](#)]
- [7] P. Ranjitha Raj, and J.S. Jayakumar, "Performance Analysis of Humidifier Packing for Humidification Dehumidification Desalination System," *Thermal Science and Engineering Progress*, vol. 27, 2022. [[CrossRef](#)] [[Google Scholar](#)] [[Publisher Link](#)]
- [8] Khalifa Zhani, "Solar Desalination Based on Multiple Effect Humidification Process: Thermal Performance and Experimental Validation," *Renewable and Sustainable Energy Reviews*, vol. 24, pp. 406-417, 2013. [[CrossRef](#)] [[Google Scholar](#)] [[Publisher Link](#)]
- [9] Adel M. Abdel Dayem, "Efficient Solar Desalination System Using Humidification/Dehumidification Process," *Journal of Solar Energy Engineering*, vol. 136, no. 4, pp. 1-9, 2014. [[CrossRef](#)] [[Google Scholar](#)] [[Publisher Link](#)]
- [10] M.T. Ghazal, U. Atikol, and F. Egelioglu, "An Experimental Study of a Solar Humidifier for HDD Systems," *Energy Conversion and Management*, vol. 82, pp. 250-258, 2014. [[CrossRef](#)] [[Google Scholar](#)] [[Publisher Link](#)]
- [11] Nabil A.S. Elminshawy, Farooq R. Siddiqui, and Mohammad F. Addas, "Experimental and Analytical Study on Productivity Augmentation of a Novel Solar Humidification-Dehumidification (HDH) System," vol. 365, pp. 36-45, 2015. [[CrossRef](#)] [[Google Scholar](#)] [[Publisher Link](#)]
- [12] Gang Wu et al., "Experimental Investigation of a Multi-Effect Isothermal Heat with Tandem Solar Desalination System Based on Humidification-Dehumidification Processes," *Desalination*, vol. 378, pp. 100-107, 2016. [[CrossRef](#)] [[Google Scholar](#)] [[Publisher Link](#)]
- [13] Farshad Farshchi Tabrizi, Meisam Khosravi, and Iman Shirzaei Sani, "Experimental Study of a Cascade Solar Still Coupled with a Humidification - Dehumidification System," *Energy Conversion and Management*, vol. 115, pp. 80-88, 2016. [[CrossRef](#)] [[Google Scholar](#)] [[Publisher Link](#)]
- [14] Mousa Abu-Arabi et al., "Experimental Investigation of a Solar Desalination with Humidification-Dehumidification Using a Rotating Surface," vol. 73, pp. 101-106, 2017. [[CrossRef](#)] [[Google Scholar](#)] [[Publisher Link](#)]
- [15] T. Rajaseenivasan, and K. Srithar, "Potential of a Dual Purpose Solar Collector on Humidification Dehumidification Desalination System," vol. 404, pp. 35-40, 2017. [[CrossRef](#)] [[Google Scholar](#)] [[Publisher Link](#)]
- [16] Sara Ladouy, and Abdelhamid Khabbazi, "Experimental Investigation of Different Air Heating Methods Near to the Evaporation Surface in Closed Triangular Shape Unit Powered by Solar Energy, One Stage - Indoor Experiment," *Applied Thermal Engineering*, vol. 127, pp. 203-211, 2017. [[CrossRef](#)] [[Google Scholar](#)] [[Publisher Link](#)]
- [17] Catalina Hernández et al., "Experimental and Numerical Evaluation of a Humidification Dehumidification Desalination Unit Driven by Solar Energy," *International Conference on Concentrating Solar Power and Chemical Energy Systems*, Santiago, Chile, vol. 2033, no. 1, 2018. [[CrossRef](#)] [[Google Scholar](#)] [[Publisher Link](#)]
- [18] Zohreh Rahimi-Ahar et al., "Comprehensive Study on Vacuum Humidification-Dehumidification (VHDH) Desalination," *Applied Thermal Engineering*, vol. 169, 2020. [[CrossRef](#)] [[Google Scholar](#)] [[Publisher Link](#)]

- [19] H. Xu, Y. Zhao, and Y.J. Dai, "Experimental Study on a Solar Assisted Heat Pump Desalination Unit with Internal Heat Recovery Based on Humidification-Dehumidification Process," *Desalination*, vol. 452, pp. 247-257, 2019. [[CrossRef](#)] [[Google Scholar](#)] [[Publisher Link](#)]
- [20] Jihane Moumouh et al., "ScienceDirect Theoretical and experimental Study of a Solar Desalination Unit Based on Humidification-Dehumidification of Air," *International Journal of Hydrogen Energy*, vol. 41, no. 45, pp. 20818-20822, 2016. [[CrossRef](#)] [[Google Scholar](#)] [[Publisher Link](#)]
- [21] A.M.I. Mohamed, and N.A.S. El-minshawy, "Humidification-Dehumidification Desalination System Driven by Geothermal Energy," *Desalination*, vol. 249, no. 2, pp. 602-608, 2009. [[CrossRef](#)] [[Google Scholar](#)] [[Publisher Link](#)]
- [22] S. Farsad, and A. Behzadmehr, "Analysis of a Solar Desalination Unit with Humidification-Dehumidification Cycle Using DoE Method," *Desalination*, vol. 278, no. 1-3, pp. 70-76, 2011. [[CrossRef](#)] [[Google Scholar](#)] [[Publisher Link](#)]
- [23] M. Capocelli et al., "Process Analysis of a Novel Humidification-Dehumidification-Adsorption (HDHA) Desalination Method," *Desalination*, vol. 429, pp. 155-166, 2018. [[CrossRef](#)] [[Google Scholar](#)] [[Publisher Link](#)]
- [24] Fahad A. Al-Sulaiman et al., "Humidification Dehumidification Desalination System Using Parabolic Trough Solar Air Collector," *Applied Thermal Engineering*, vol. 75, pp. 809-816, 2015. [[CrossRef](#)] [[Google Scholar](#)] [[Publisher Link](#)]
- [25] A.E. Kabeel, and Emad M.S. El-Said, "Experimental Study on a Modified Solar Power Driven Hybrid Desalination System," *Desalination*, vol. 443, pp. 1-10, 2018. [[CrossRef](#)] [[Google Scholar](#)] [[Publisher Link](#)]
- [26] A. Fouda, S.A. Nada, and H.F. Elattar, "An Integrated A/C and HDH Water Desalination System Assisted by Solar Energy : Transient Analysis and Economical Study," *Applied Thermal Engineering*, vol. 108, pp. 1320-1335, 2016. [[CrossRef](#)] [[Google Scholar](#)] [[Publisher Link](#)]
- [27] Mahmoud Shatat et al., "Theoretical Simulation of Small Scale Psychometric Solar Water Desalination System in Semi-arid Region," *Applied Thermal Engineering*, vol. 59, no. 1-2, pp. 232-242, 2013. [[CrossRef](#)] [[Google Scholar](#)] [[Publisher Link](#)]
- [28] Emily W. Tow, and John H. Lienhard, "Experiments and Modeling of Bubble Column Dehumidifier Performance," *International Journal of Thermal Sciences*, vol. 80, pp. 65-75, 2014. [[CrossRef](#)] [[Google Scholar](#)] [[Publisher Link](#)]
- [29] Y.J. Dai, R.Z. Wang, and H.F. Zhang, "Parametric Analysis to Improve the Performance of a Solar Desalination Unit with Humidification and Dehumidification," *Desalination*, vol. 142, no. 2, pp. 107-118, 2002. [[CrossRef](#)] [[Google Scholar](#)] [[Publisher Link](#)]
- [30] M.G. Morsy, I.M. Ismail, and Ali M.A. Soliman, "Experimental Performance of Spray Type Humidifier in Humidification-Dehumidification Desalination Unit," *Journal of Engineering Sciences*, vol. 37, no. 6, pp. 1433-1447, 2009. [[CrossRef](#)] [[Google Scholar](#)] [[Publisher Link](#)]
- [31] G. Prakash Narayan et al., "Thermal Design of the Humidification Dehumidification Desalination System: An Experimental Investigation," *International Journal of Heat and Mass Transfer*, vol. 58, no. 1-2, pp. 740-748, 2013. [[CrossRef](#)] [[Google Scholar](#)] [[Publisher Link](#)]
- [32] T. Rajaseenivasan et al., "Combined Probation of Bubble Column Humidification Dehumidification Desalination System Using Solar Collectors," *Energy*, vol. 116, pp. 459-469, 2016. [[CrossRef](#)] [[Google Scholar](#)] [[Publisher Link](#)]
- [33] S. Eiamsa-ard et al., "Heat Transfer Enhancement in a Tube Using Delta-Winglet Twisted Tape Inserts," *Applied Thermal Engineering*, vol. 30, no. 4, pp. 310-318, 2010. [[CrossRef](#)] [[Google Scholar](#)] [[Publisher Link](#)]
- [34] Smith Eiamsa-ard et al., "Convective Heat Transfer in a Circular Tube with Short-Length Twisted Tape Insert," *International Communications in Heat and Mass Transfer*, vol. 36, no. 4, pp. 365-371, 2009. [[CrossRef](#)] [[Google Scholar](#)] [[Publisher Link](#)]
- [35] Iraj Ghofrani, and Ali Moosavi, "Energy , Exergy , Exergoeconomics , and Exergoenvironmental Assessment of Three Brine Recycle Humidification-Dehumidification Desalination Systems Applicable for Industrial Wastewater Treatment," *Energy Conversion and Management*, vol. 205, 2020. [[CrossRef](#)] [[Google Scholar](#)] [[Publisher Link](#)]
- [36] Weifeng He, Hongxing Yang, and Dong Han, "Thermodynamic Investigation and Optimization of a Heat Pump Coupled Open-Air, Open-Water Humidification Dehumidification Desalination System with a Direct Contact Dehumidifier," *Desalination*, vol. 469, 2019. [[CrossRef](#)] [[Google Scholar](#)] [[Publisher Link](#)]
- [37] S.P. Sukhatme, "Can India's Future Needs of Electricity be Met by Renewable Energy Sources ? A Revised Assessment," *Current Science*, vol. 103, no. 10, pp. 1153-1161, 2012. [[Google Scholar](#)] [[Publisher Link](#)]

- [38] Cemil Yamalı, and İsmail Solmuş, "Theoretical Investigation of a Humidification-Dehumidification Desalination System Configured by a Double-Pass Flat Plate Solar Air Heater," *Desalination*, vol. 205, no. 1-3, pp. 163-177, 2007. [[CrossRef](#)] [[Google Scholar](#)] [[Publisher Link](#)]
- [39] T.L. Bergman et al., *Fundamentals of Heat and Mass Transfer*, 7<sup>th</sup> ed., John Wiley & Sons, 2011. [[Google Scholar](#)] [[Publisher Link](#)]
- [40] Yan Huang et al., "Progress on Polymeric Hollow Fiber Membrane Preparation Technique from the Perspective of Green and Sustainable Development," *Chemical Engineering Journal*, vol. 403, 2021. [[CrossRef](#)] [[Google Scholar](#)] [[Publisher Link](#)]
- [41] Xiangjie Chen et al., "Experimental Investigation of a Polymer Hollow Fibre Integrated Liquid Desiccant Dehumidification System with Aqueous Potassium Formate Solution," *Applied Thermal Engineering*, vol. 142, pp. 632-643, 2018. [[CrossRef](#)] [[Google Scholar](#)] [[Publisher Link](#)]
- [42] Guo-Pei Li, and Li-Zhi Zhang, "Investigation of a Solar Energy Driven and Hollow Fiber Membrane-Based Humidification-Dehumidification Desalination System," *Applied Energy*, vol. 177, pp. 393-408, 2016. [[CrossRef](#)] [[Google Scholar](#)] [[Publisher Link](#)]
- [43] I. Budihardjo, and G.L. Morrison, "Performance of Water-in-Glass Evacuated Tube Solar Water Heaters," *Solar Energy*, vol. 83, no. 1, pp. 49-56, 2009. [[CrossRef](#)] [[Google Scholar](#)] [[Publisher Link](#)]
- [44] Sulaiman Al-Obaidani et al., "Potential of Membrane Distillation in Seawater Desalination : Thermal Efficiency, Sensitivity Study and Cost Estimation," *Journal of Membrane Science*, vol. 323, no. 1, pp. 85-98, 2008. [[CrossRef](#)] [[Google Scholar](#)] [[Publisher Link](#)]
- [45] M.A. Darwish, and Najem M Al-Najem, "Energy Consumption by Multi-Stage Flash and Reverse Osmosis Desalters," *Applied Thermal Engineering*, vol. 20, no. 5, pp. 399-416, 2000. [[CrossRef](#)] [[Google Scholar](#)] [[Publisher Link](#)]
- [46] S. Bouguecha, B. Hamrouni, and M. Dhahbi, "Small Scale Desalination Pilots Powered by Renewable Energy Sources : Case Studies," *Desalination*, vol. 183, no. 1-3, pp. 151-165, 2005. [[CrossRef](#)] [[Google Scholar](#)] [[Publisher Link](#)]
- [47] A.S. Nafey, H.E.S. Fath, and A.A. Mabrouk, "Thermo-Economic Investigation of Multi Effect Evaporation (MEE) and Hybrid Multi Effect Evaporation - Multi Stage Flash (MEE-MSF) Systems," *Desalination*, vol. 201, no. 1-3, pp. 241-254, 2006. [[CrossRef](#)] [[Google Scholar](#)] [[Publisher Link](#)]
- [48] Muhammad Tauha Ali, Hassan E.S. Fath, and Peter R. Armstrong, "A Comprehensive Techno-Economical Review of Indirect Solar Desalination," *Renewable and Sustainable Energy Reviews*, vol. 15, no. 8, pp. 4187-4199, 2011. [[CrossRef](#)] [[Google Scholar](#)] [[Publisher Link](#)]
- [49] H. Müller-Holst et al., "Solarthermal Seawater Desalination Systems for Decentralized Use," *Renewable Energy*, vol. 14, no. 1-4, pp. 311-318, 1998. [[CrossRef](#)] [[Google Scholar](#)] [[Publisher Link](#)]
- [50] Hossam A. Ahmed et al., "Experimental Investigation of Humidification-Dehumidification Desalination System with Corrugated Packing in the Humidifier," *Desalination*, vol. 410, pp. 19-29, 2017. [[CrossRef](#)] [[Google Scholar](#)] [[Publisher Link](#)]